

We are IntechOpen, the world's leading publisher of Open Access books Built by scientists, for scientists

5,600

Open access books available

137,000

International authors and editors

170M

Downloads

Our authors are among the

154

Countries delivered to

TOP 1%

most cited scientists

12.2%

Contributors from top 500 universities



WEB OF SCIENCE™

Selection of our books indexed in the Book Citation Index
in Web of Science™ Core Collection (BKCI)

Interested in publishing with us?
Contact book.department@intechopen.com

Numbers displayed above are based on latest data collected.
For more information visit www.intechopen.com



Focal Increased Radiopharmaceutical Uptake Differentiation Using Quantitative Indices

V. Sivasubramaniyan and K. Venkataramaniah

Abstract

Focal increased radiopharmaceutical uptake in a lesion results in focal Hot Spots in the scans. This can occur in benign infective or inflammatory disorders and cancerous diseases as well. Comparison between malignant and benign lesions is important. The Hot spots can be classified into benign and malignant lesions by Spatial Scintimetry or Temporal Scintimetry. Spatial Scintimetry compares the uptake in the region of interest with the adjacent tissue or the unaffected contralateral site. The quantitative indices are lesion/non lesion ratio, lesion/background activity and lesion to Bone ratio etc. The Temporal Scintimetry relies on the changes in the counts or uptake in the Hotspot lesion with reference to the dual point time of acquisition. The Hotspot in the bone scan can be classified using the quantitative index of retention ratio by Dr. V. Siva and Israel. In PET studies the focal hot spots can be differentiated into benign and malignant lesion using the dual phase PETCT evaluation using the Rong's Retention ratio and Dr. V. Siva's modified RRI values.

Keywords: radiopharmaceutical uptake, scintimetric characterization, spatial scintimetry, temporal scintimetry, quantitative indices

1. Introduction

The uptake of the Radiopharmaceuticals in the organ of interest makes the functional evaluation of that organ feasible. Not only that the radiopharmaceutical uptake in the pathological conditions depends on the blood supply to the organ, bolus injection of the radiopharmaceutical and the functional integrity of the organ. When there is increase in blood supply and integral functionality in a lesion will lead to focal increase in radiopharmaceutical uptake resulting in the Hot spots. In those situations where there is reduction in the blood supply to the organ and decreased functional integrity will result in photopenic or photon void lesions. Conventionally scintigraphic imagery is being inferred by graphical inspection of the photographic imprints and comparing with the known normal distribution pattern in the organ of interest.

The advancement of digital scanning technologies have made it easier to measure the scintillations by quantifying the per pixel counts of the intended regions. In addition, the post-processing and PACS transmission characteristics have been the

major reason behind the Dicom compatible graphics. The phrase “SCINTIMETRY” means the number of scintillations taking place in intended regions in scintigraphic imagery that has been covered in the study. Basically, “Scintimetry” is the combined term of “Scintillation + Metric”.

2. Scintimetric characterization

The scintillations in a focal hot spot can be counted using Scintimetry. Depending upon the method of comparison there are TWO types of Scintimetry:

1. Regional: The process of drawing the region of interest (ROI), picking the ROI, and comparing the same with either equivalent or neighboring site on the contra lateral part by marking the same region of interest is known as Spatial Scintimetry.
2. Temporal: The ROI is drawn above the lesion of interest or the site at a time and evaluating the same with a region of interest on the acquired imagery after some time from the first study is known as “Time Bound Scintimetry” or the scintimetry of same ROI regarding time.

2.1 Regional scintimetry methods

Scintimetric evaluations can be performed with several quantitative approaches. Some of the most popular methods are: a. Local Uptake; b. bone soft tissue ratio; c. Lesion bone ratio; d. Standardized Uptake Ratio (SUV); and e. Percentage uptake.

- a. Local uptake ratio: It is the easiest way to quantify the tracer’s uptake in an ROI to determine the count rate calculated in the form of ratio of count rate in a region in a closest area in identical image (Rosenthal and Kaye, 1975) [1]. On the other hand, it is also possible to use a line profile curve at lesion area (Lentle et al., 1977) [2], **Figure 1**.
- b. Lesion Bone (L/B) Ratio: Here, “lesion” means focal region of abnormality and “bone” refers to the suitable region of a bone. Its utility has been best described by (Condon et al., 1981) [3] and (Vellenga et al., 1984) [4] when it comes to detect rib lesions and almost indiscernible lesions.

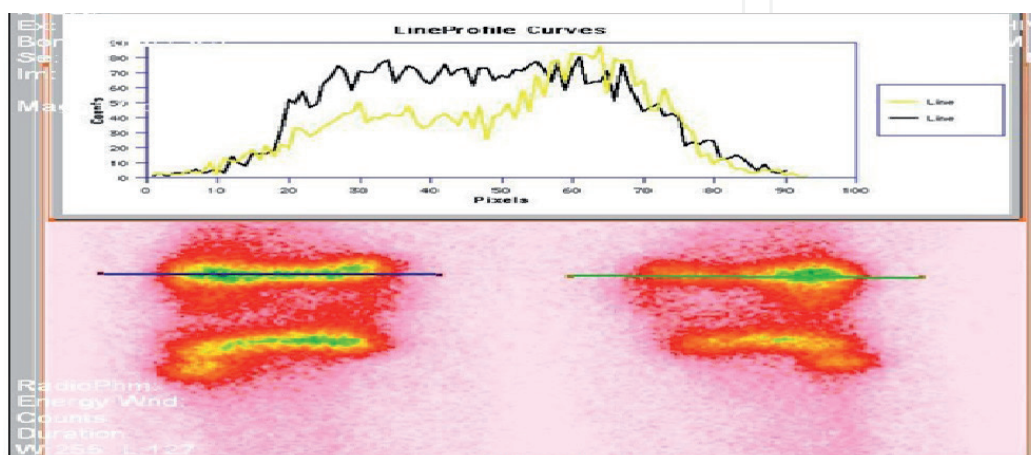


Figure 1.
Line profile curve.

- c. Bone/Soft Tissue: There are some measurements that can help detect hematological malignancies in patients (Pfeifer et al., 1983) [5]. This ratio has been used by (Constable and Cranage, 1980) [6] to verify the prostatic super scans.
- d. Percentage uptake: The uptake is referred in the area of interest to the given dose to calculate the percentage uptake (Hardly et al., 1980) [7] or to the given external activity by Meindok et al., 1985 [8].

2.2 Methods of temporal scintimetry

There are two methods to do it:

- a. Retention Ratio and
- b. Change in the regional uptake ratios with reference to time.
 - Retention Ratio: Israel et al., 1985 [9] measured Lesion Bone uptake with this clue at 4 and 24 hours and suggested that the ratio of 24/4-h was lower among patients who have been through metastasis treatment and who have degenerative disease. Dr. V. Siva et al., 1995 [10] devised a retention ratio of 4/24 hr. to distinguish the focal hotspots into Metabolic, Benign, and Malignant characteristics. In that study it has been demonstrated that the Retention ratio 0–5 indicates benign nature of the lesion, 5–10 denotes indeterminate or metabolic or degenerative nature and 10 and above confirms the malignant nature of the lesions. The concept is being depicted in **Figure 2**.
 - Change in Regional uptake ratio: The change in the Regional uptake ratio with reference to time is currently used in the evaluation of healing potential of Fracture neck of Femur [10].

3. Scintimetric classification of skeletal hot spot in bone scan

X-ray is not sufficient to diagnose bone metastases. Nuclear scintigraphy imaging has always been helpful for early diagnosis of bone disease. The diphosphonates

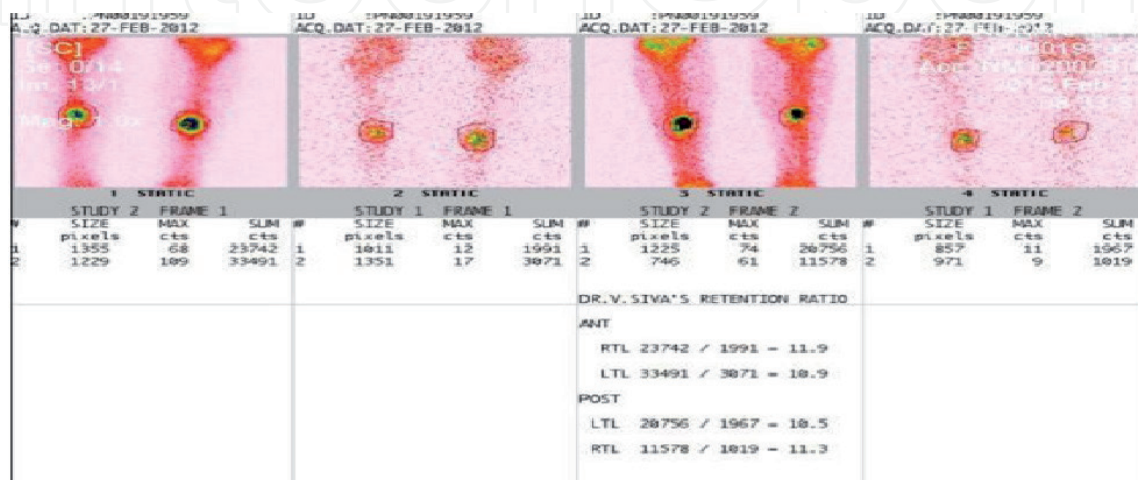


Figure 2.
 Dr. V. Siva's retention ratio.

labeled as “^{99m}Tc” in Bone scan detects the osteoblastic response that takes place in malignant cells. This method is best suited for the entire body scan at affordable cost and with high sensitivity and availability. But there is a problem with specificity [11]. The crystal immature bone surfaces absorb the “^{99m}Tc-polyphosphate” along with its variants through ionic deposition.

The rise in bone vascularity raises this process along with matrix localization. Hence, the focal hotspots or abrupt scintiscan area is the region of elevated osteoblastic activity. The Scintiscan bone has been shown to be more sensitive than x-rays to detect bone’s focal illness. The major flaw in this process is the non-specificity of the study [12].

There are reasons Prostatic Carcinoma metastasis, which is usually found in bone, has gained a lot of attention for investigation. The anatomical aspects of the prostate gland are the first reason. Baston’s plexus is the venous drainage of the prostate gland with a unique range of venous plexus. The Lumbosacral plexus of veins is directly connected with it. In the advanced stage of prostate cancer, this metastatic lesion occurs especially in the axial skeleton [13].

It is not possible to cover the metastatic association in ribs, skull and the bones with this anatomical elaboration. According to Paget, there have been mutations in carcinoma prostate cells in osteotropic cells either with activation of particular proteases and cytokine or with genetic form. They can be latent till an expected change takes place around them like a seed. Hence, there is some clue in the ‘seed and soil’ theory from the next standpoint [14]. The elevated levels of TGF- β and “bone morphogenetic proteins (BMPs)” had been established in metastasis of bones in prostate cancer cells [15–18]. These cells of “osteotropic metastatic seeds” are combined to the endothelium of bones better than other tissues’ endothelium [19].

The skeletal tissue contains Tc-99 mm MDP as the ionic radiopharmaceutical radius is much like the same of “Calcium Hydroxy-appetite crystal”. Hence, it is added to the skeletal tissue. Hence, even Osteomyelitis, Paget’s disease and Post Traumatic skeletal disorders occur with focal skeletal hotspots. For skeletal hotspots, the major cause must be determined with invasive procedure and further scanning as well. Several quantitative measures are there to improve the specificity of bone scan. Along with fusion imaging procedures like PET-CT and SPECT-CT, BONE SPECT and other cross-sectional techniques have been introduced. We have proposed a novel Scintimetric technique in this work for bone scanning to verify and rule out metastatic or malignant nature of skeletal areas in the non-invasive bone imaging.

The bone scans have focal hotspot margins of 4 and 24 h followed by injecting radiopharmaceutical drawings with a tool and experts tabulate the maximum per-pixel counts in such scans. The ratio of two values is taken to determine the focal hotspot changes in the scan with time interval. It is defined as Scintimetry of one region regarding time and is termed “Time Bound Scintimetry”. In addition, it is possible to infer the metabolic turnover in hotspots.

4. Temporal scintimetry method and Dr. Siva’s retention ratio

A method named “Temporal Scintimetry” has been proposed by Israel et al. [9]. The Non lesion (NL) and Lesion (L) count ratio has been measured over the bone at 4 h in bone imaging. It is also performed again in bone scan at 24 h as well.

$$\text{“Israel’s ratio} = L / N_{24 \text{ h}} / L / N_{4 \text{ h}} \text{”} \quad (1)$$

There has been too negligible variation in measurements among patients who have been treated with metastasis and with degenerative disease and it was steep in metastatic lesions. The decimal values came up in the result only as the indicator is high according to the “Radioactive decay law”. We also presented Dr. V. Siva’s 4/24 h retention ratio in this work to classify the ‘focal hot spots’ and to find the difference between benign lesions and metastatic lesions with this procedure [10]:

1. Only the maximum counts at the Lesion or Focal hot spot were taken rather than L/N ratio.
2. The 4/24 h ratio of Dr. V. Siva is taken rather than Israel’s 24/4 h ratio.

5. Dr. V. Siva’s retention ratio = 4/24 h focal hot spot count

5.1 Clinical applications of scintimetric characterization of the skeletal hotspots in the differentiation of benign and metastatic lesion

The bone scan was performed 4 h following the 15–25 mCi of IV injection containing “Tc-99 m Methylene Di-Phosphonate “with proper hydration with the entire body acquisition of dual head gamma camcorder of Siemen’s eCAM. Next day, the full-body bone imaging is done again with the same protocol and injection. The General Display protocol is used to select both images of 4 h and 24 h. The 4 h anterior and 24 h posterior scans are selected with Region Ratio protocol and the experts tabulate the maximum counts at a focal area. The region ratio protocol is used to calculate Dr. V. Siva 4/24 h retention ratios and it is also tabulated.

In a study, a group of 32 patients with proven and known Paget’s disease, Avascular Necrosis, Osteomyelitis, and degenerative problems and 75 patients with proven Carcino Prostate biopsy reports were included. There was metastatic involvement in 53 people in a Carcinoma Prostate group, out of which 22 were reported negative for metastases. The “ 11.5 ± 2.8 ” is the mean value of the 4/24 retention ratio of Dr. V. Siva in malignant bone lesions and “ 0.08 ± 0.02 ” is the mean value of Israel’s 24/4 ratio in the group with Carcinoma Prostate. The mean value of “ 4.8 ± 2.5 ” was found in benign bone lesions in Dr. V Siva’s 4/24 retention ratio and “ -0.06 ± 0.02 ” was the mean value of Israel’s 24/4 ratio. The statistical values are estimated using the online “Social Sciences Statistics” calculator. The T value comes out to be 17.1 from the two independent values of the student T test. There was a significant result at $p < 0.05$ value and < 0.00001 is the p value. There was a significant outcome at $p < 0.05$ value. **Figure 3** illustrates the graphical calculation of dispersion and major difference between metastatic and benign lesions:

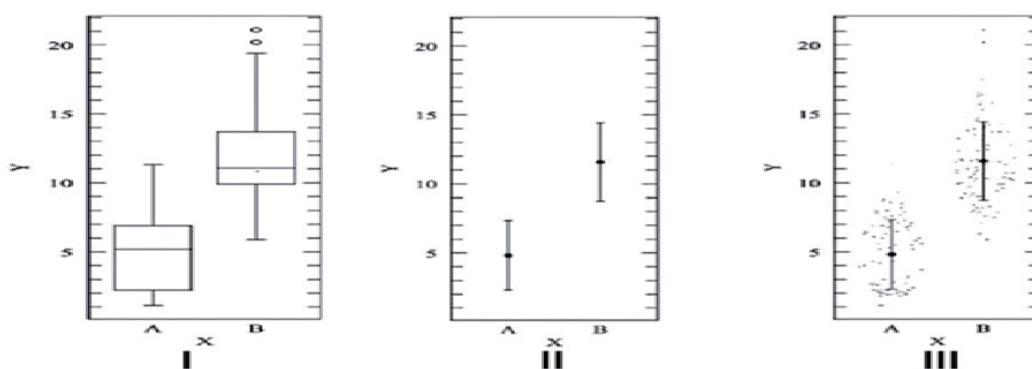


Figure 3.
 The graphical representation of difference between A – Benign and B – Malignant lesions.

The Quantitative and non-invasive classification of “Skeletal Metastasis” with Tc99m MDP scans in Carcinoma prostate was presenting good values with Retention Ratio of Dr. V. Siva as per Serum PSA levels [20].

6. Evaluating pathological/non-healing fractures using scintimetry

The authors in [21] have documented the “Scintimetric” assessment of “delayed union of skeletal fractures”. The retention values of 4/24 for all cases were characterized into benign fracture and metastatic fracture as per the scintometric classification of skeletal hot spots. Around 37% (11) were pathological fractures and 63% (19) were benign ones due to benign bone tumors and stress fracture out of 30 non-union/delayed skeletal fractures reported. Dr. V. Siva’s 4/24 h retention ratio had 12.5 ± 3.1 of mean value for pathological group with typical estimation of ± 0.61 for errors and the error estimation (± 0.38) was measured with mean value “ 6.68 ± 2.8 ” of benign group. The statistical calculation found a major difference between two values with <0.0001 of p value.

The authors in [22] also reported the comparative study of Scintimetric classification by the “Triple Phase Bone Scan” and Retention Ratio by Dr. V Siva in skeletal fracture as compared to the entire body counts. The authors in [23] also described the use cases of “scintometric classification of skeletal hotspots” also in a diagnostic facility.

7. Scintimetry in rheumatoid arthritis

The bone imaging of two-sided hands is helpful to determine the severity of afflictions in interphalangeal joints. The accumulation of delayed 24 h imaging of hands and quantitative retention ratio measurements was helpful. The authors in [24] also published a groundwork report on Scintimetric assessment of the involvement of rheumatoid arthritis by retention ratio of Dr. V Siva. The mean of “ 5.91 ± 0.35 ” was found in the maximum counts of skeletal zones of patients in 3 h and 24 h scans as well as the 4/24 h ratio with means of 0.3496 in standard error. The 8.8408 was the estimated variance and 2.9734 was the standard and estimated deviation. The 6.6306 was the estimated variance for the sample size and 2.575 was the standard estimated deviation by modification from HOJO. The sample population was very small and it was totally unavoidable. It opens further research paths on a global scale.

8. Diastolic dysfunction assessment, characterization and identification

The left ventricle has the diastolic function that plays an important role in efficacy and preservation of left systolic ventricular function. Hence, there have been a lot of concerns on determining the “Left Ventricular Diastolic function” as well as the management and detection of left heart failure. The “M-mode echocardiography” is usually taken to evaluate the same at the mitral valve orifice with “E/A ratio” tracing. The “Left Ventricular Diastolic function” Stage I is represented by <0.8 of E/A ratio, Stage II by >1.4 , and Stage III by >1.8 [25, 26]. The tissue characterization and “Color Doppler echocardiography” are the methods to refine these parameters [27].

The advancement of studies related to “ECG-Gated SPECT” has given great insights for its evaluation. The visual insights to “Regional Wall Motion Abnormalities” and “Ejection Fraction” with “Gated SPECT Myocardial Perfusion Studies” are widely used and popular. However, it is still important to explore

the portal to extract and analyze vital info from the analysis of “Phase image” of systolic and diastolic phases in cardiac cycle. After the use of “Gated SPECT Myocardial Perfusion Imaging” described by Morgan and Mannting [28] in the year 1993, Raymond Taillefer et al. [29] explained the “Diastolic image analysis” and its utility in early diagnosis of C.A.D. among women over “Summed Image Analysis” in the year 1999.

A “Gated SPECT Perfusion Processing” protocol has been developed by Siemens on the basis of Depuey et al. [30] who have covered individual image analysis in “Ejection fraction calculation”, “Diastole and Systole”, and “Regional Wall Thickness”. With “phase image analysis” in processing of “Gated SPECT Perfusion”, the “Irregular, In-homogenous, and Insufficient Tracer distribution” incidence is inferred having regular, homogenous and even tracer distribution in summed scans to show diastolic dysfunction. The “SNMICON” presentation [31] also highlights the association with the markers of “echocardiographic diastolic dysfunction”, especially “Diabetes Mellitus and Hypertension” and E/A ratio.

The ideal correlation between S/D ratio and rate of Peak flow is estimated by considering the “Time Volume” curves that are obtained from E/A ratio and ECG-gated SPECT [32]. The “Time To Peak Flow” and “Peak Flow Rate” are the parameters of diastolic dysfunction. Their normal values have been documented to determine diastolic function with total agreement between “Echocardiographic assessment and QGSPECT” using 16-frame “99mTc-Sestamibi Gated Myocardial Perfusion SPECT” [33]. According to RD Lele et al., diastolic dysfunction was 92/121 (76) and “echocardiographic E/A ratio” detected only 53/121 (43%) [29]. The common individual risk factor was “Left Ventricular Hypertrophy (LVH)” with heavy risk related to unfavorable results [34, 35]. Some of the major causes are hypertension and hypertrophic cardiomyopathy (HCM) [36] and aortic stenosis, obesity, and chronic kidney problems are responsible for the thickness of the left LV wall [37–40].

There were 75 males aged 31 to 67 years participated in a study to evaluate the left “ventricular diastolic dysfunction” with average age of 51.9 ± 7.4 years and there were 25 females from 31 to 55 years with mean 45.9 ± 6.6 years of mean age. The patients using “Thallium-201 Bruce protocol 2-mCi” on a treadmill were injected after exercise with “Gated SPECT MPI” through IV. They were equipped with E-Cam Dual Head Gamma cam by Siemens. The “Gated SPECT PERFUSION ANALYSIS” protocol was used by the ICON software to analyze the images. The irregular, in-homogenous and insufficient tracer distribution was found in diastolic phase scans instead of usual Systolic phase scans. These images show changes in diastolic dysfunction in “left ventricular muscle tissue” (Figure 4).

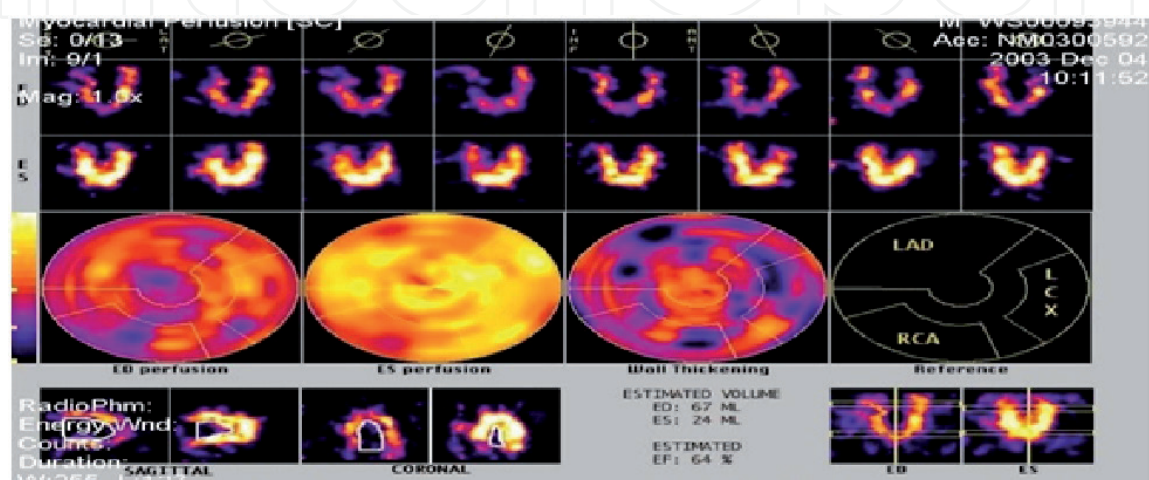


Figure 4.
Diastolic images – Upper row, systolic images middle row, Bull's eye maps third row.

The images on the upper row show diastolic phase in various angles. These scans show in-homogenous, constantly decreased, irregular, and insufficient distribution of tracer, which indicate perfusion absence. The images on the lower row of the systolic phase illustrate stable and normal tracer distribution. In this study, the discordance between systolic and diastolic phases has been displayed and it is related to straight changes because of diastolic dysfunction in the “left ventricular muscle mass”. These images display Bull’s eye map assessment and ‘left ventricular ejection fraction’ of the end systolic perfusion, end diastolic perfusion, and wall thickening. The systolic and diastolic phases are described in the images on the lower and upper row, respectively. The bull’s eye map of “diastolic phase ED perfusion” describes affliction from moderate to severe levels as per the ES perfusion on systolic phase and color scale that displays color and normal scale. The left ventricular ejection fraction which is calculated from the “end systolic ES volumes” and derived end diastolic ED” is normal.

The research findings have been noted as below. The researchers have tabulated the echocardiographic grading of “left ventricular diastolic dysfunction” apart from the findings given above. They saved the scan data of systolic and diastolic pictures in H.L.A., S.A., and V.L.A. views. The inner and outer margins are drawn by the “ventricular wall outline” in the systolic and diastolic phase and counts were calculated in the area of interest with the ICON software’s region ratio count protocol (**Figure 5**).

The S/D ratio was used to tabulate the diastolic and systolic counts in female and male patients in this study. We also analyzed the S/D ratios of diastolic dysfunction stage II and Stage III individually. We found the discordance between systolic and diastolic pictures in 98/100 (98%). The Grade II and Grade III classify the echocardiographic images of this disorder with E/A ratio in 87/100 (87%). Similarly, hypertension was reported in 63% and diabetes in only 16%. There was no major statistical change in S/D ratio between both groups (**Figure 6**).

The Grade II LVDD has 1.47 ± 0.32 of S/D ratio and Grade III LVDD has 1.81 ± 0.03 of S/D ratio. With “Paired Student t-test”, the statistical data found a major difference between Stage II and Stage III in S/D ratio (**Figure 7**).

The visual analysis of the images of systolic and diastolic phases led to interpretation and identification of heart’s “Left ventricular diastolic dysfunction”. This method identified 98% (98/100) people with this condition. On the other hand, the E/A echocardiographic test detected only 87% of patients. The direct changes

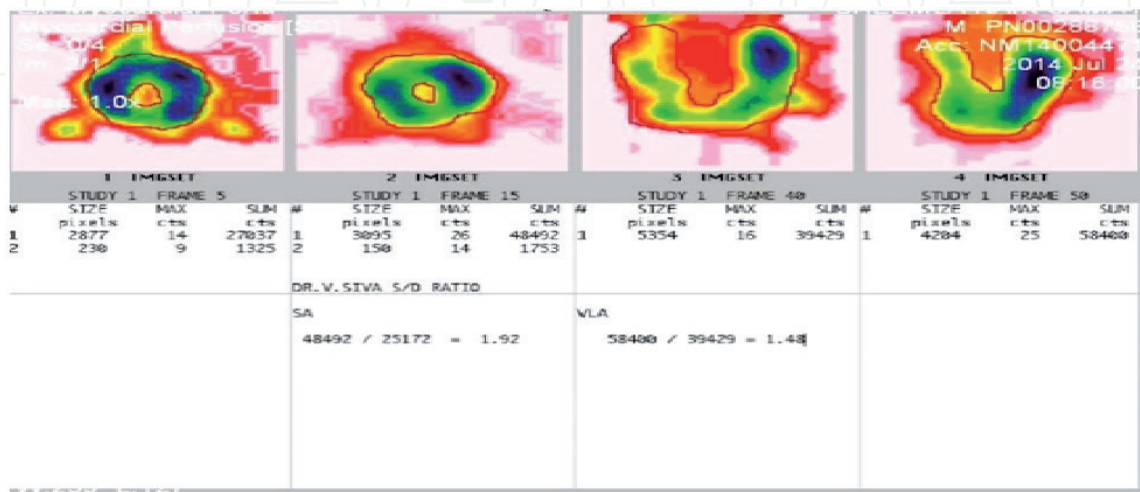


Figure 5. Scintimetric method of calculating Distolic and systolic for deriving S/D ratio.

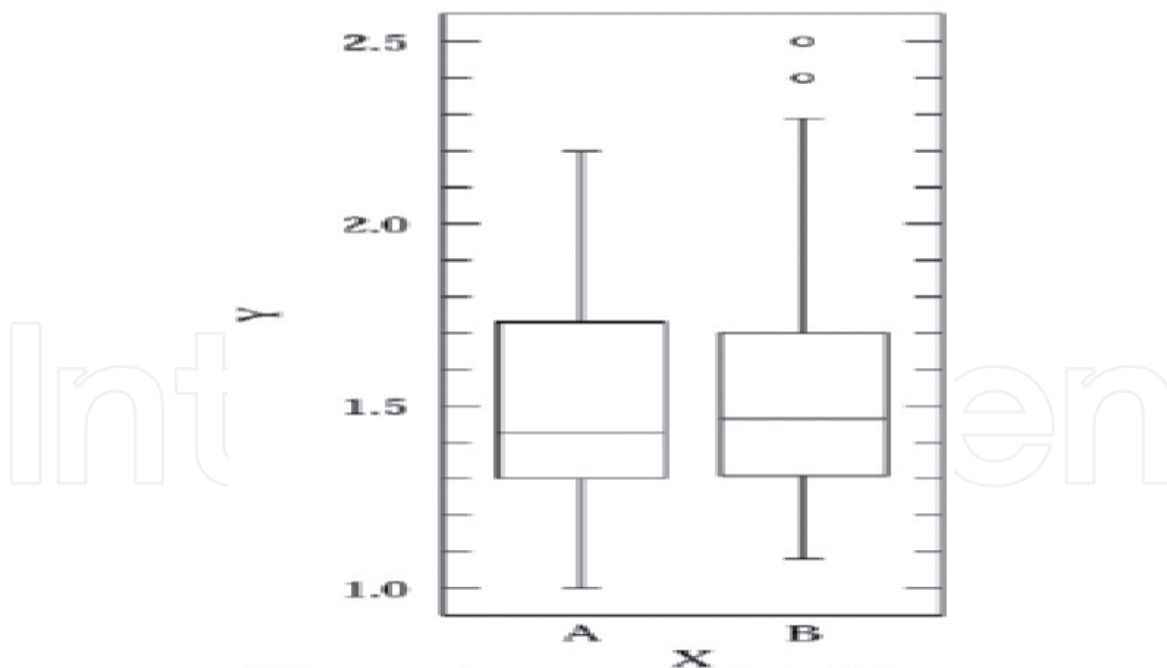


Figure 6.
No difference between A-male and B-female scintimetric S/D values.

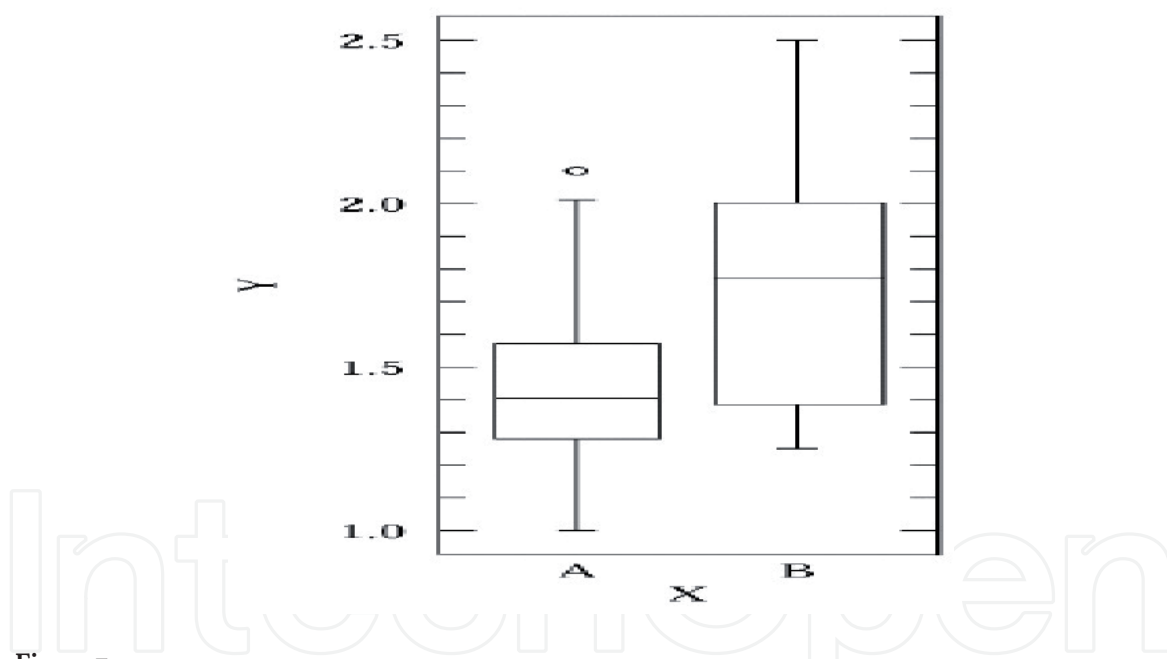


Figure 7.
Significant difference between A-stage II and B-stage III scintimetric S/D values.

in “Left ventricular cardiac myocytes” base the visual analysis to diagnose diastolic dysfunction. Hence, they could detect 98% of cases with diastolic dysfunction. RD Lele et al. [34] detected only 76% (92/121) cases with diastolic heart function by using “16-Gated Myocardial Perfusion SPECT” and “time volume curve” analysis.

On the other side, diastolic dysfunction is detected in 98% patients with “direct visual image interpretative assessment” of systolic and diastolic phases. However, there is a need to extend this study further to all the rest of “Gated SPECT” research for a large number of patients. It is also important to contemplate the separated comparison of ES and ED perfusions in both rest and stress gated myocardial imaging results. Along with it, the normal population should also be included as this study group covered only patients.

9. Scintimetric characterization of primary tumors by dual phase PETCT study

The utility and advantage of the dual phase PETCT evaluation in the tumor detection was reported by Kuboto K et al. [41]. The optimal time interval between the early and delayed phase PETCT scans had been proved to be 3 hr. post injection by Chen YM et al. [42]. In our study protocol the delayed PETCT was conducted at 4 hours post injection due to logistic reasons. Rong et al. reported a quantitative estimation to differentiate between the benign and malignant bone lesions using the dual phase PETCT evaluation termed as Rong's Retention Index [43]. The Rong's retention index (RRI), computed as follows:

$$\text{RRI} = (\text{SUV}_{\text{maxD}} - \text{SUV}_{\text{maxE}}) \times 100 \quad (2)$$

Even though there is a noticeable difference between the malignant and benign bone lesions, they also have a major overlap in between.

$$\text{Dr.V.Siva's modified Retention ratio} = \frac{\text{SUV}_{\text{max Delayed}}}{\text{SUV}_{\text{max Early}}} \times 100 \quad (3)$$

We have focused on the clinical and technical aspects of a novel method in this oncologic utility of "Positron Emission Tomography (PET)". In this method, the PET scanner is combined with a CT scanner in a single device [44–47].

In May 2019, this study was conducted among 19 patients aged 9 to 76 years (12 females, 7 males) with a median of 46 ± 18 years with active primary and metabolically lesions of several types of cancers. Permission was taken from each volunteer before they joined the study for delayed 4 h PET/CT scan without injecting F18-FDG any further. The protocol of "F-18 FDG PET image reconstruction and acquisition" was approved by the ethics group and all cases have obtained official consent.

Patients did not drink or eat anything for 4 to 6 hours before IV injection of "F-18 FDG (185 to 375 MBq, i.e. 4 MBq/kg of weight of the body)". Before getting injected, patients received the concentration of serum glucose and all patients had glucose levels below 200 mg/dl. After the injection at 1 hour early and PET/CT scans at 4 hour (delayed) after injection with PET/CT scanner (from PETCT and Wipro GE), the patients settled down in a silent room. The Spiral CT was used for acquiring CT image at 0.75 s per rotation with 4 mm of section thickness, 4 mm of interval, and 40mAs and 120 kVp.

No IV contrast injection was used. We obtained the early images of PET emission from thigh to cranium, usually with 6–7 positions with acquisition of 2 minutes in each bed position. We acquired the images of delayed PET emission of abnormal spots at 4 h after F-18 FDG injection, with 2 minutes of interval between 2 to 3 bed positions. We used the LOR algorithm to reconstruct all PET scans while applying CT-based correction of attenuation. We used the "Advantage 4.7 Volume Viewer" program to obtain the images. The F-18 FDG uptake was evaluated with delayed and early PET images, evaluation of parameters and interpretation of PET image, semi quantitatively. A circular ROI was positioned above the detected bone lesion for semi-quantitative analysis with transverse PET picture.

The ROI was positioned above the whole "F18 FDG lesion" for visualized lesions on PET, including utmost radioactivity. The following formula was used to estimate the "Standardized Uptake Value":

$$\text{"SUV} = \text{tissue concentration (MBq/g)} / [\text{injected dose (MBq)} / \text{body weight (g)}\text{"}$$

For each region of interest, the SUVmax or maximal SUV was calculated in lesion ROI. The variations in the lesions' uptake were measured as retention index:

$$\text{“RI} = (\text{SUVmaxD} - \text{SUVmaxE}) \times 100 / \text{SUVmaxE} \text{”} \quad (4)$$

Here is the formula to calculate RRI modification by Dr. V. Siva:

$$\text{“RRI} = \text{SUVmaxD} / \text{SUVmaxE} \times 100 \text{”} \quad (5)$$

The dual time point based quantifications of metabolic uptake rate in 18F-FDG PET had been reported by den Hoff et al. [48]. The potential diagnostic role of dual phase 18F-FDG PETCT scanning was reported by Jones c et al. [49]. This is the first study reporting the findings of the dual phase PETCT in the evaluation and characterization in various primary lesions. The Rong's Retention values showed a wide ranging value and no definite cut off value could be arrived at. But Dr. V. Siva's modification of Rong's Retention Ratio revealed that the cut off value to be 100 and above for confirming the malignant nature of the lesions. The statistical evaluation of the values by Student t Test showed good p value confirming the significance that the two values were significantly different. There is a strong positive correlation in the "Pearson evaluation". It means a high y variable with high x scores and vice versa (**Figure 8**). The inclusion of the various primary malignancies in both the sexes adds advantage to the study. However the non-inclusion of primary benign lesions in the study is the greatest disadvantage. The other limitations being the single institutional study and the small number of patient population.

Scintimetric Characterization of metastatic lymph nodes in various primary malignancies by Dual Phase PETCT study.

In the proven cases of various primary malignancies like Ca. Breast, Ca. Prostate, Lymphomas and alveolar tumors the SUV max values of the metastatic lymph nodes were calculated in both the Early and Delayed phase scans. The PETCT study was performed using the GE Discovery IQ PETCT in those patients with positive lymph node uptake. The early scan was done One hour post injection of 5 to 10 mCi of F18-FDG tracer in the fasting state with their informed consent with optimal serum blood

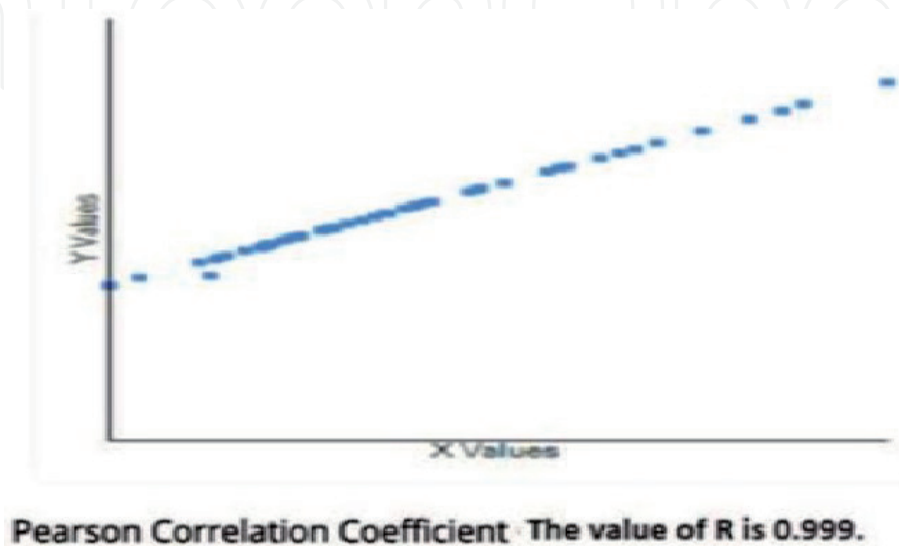


Figure 8.
Pearson correlation coefficient test.

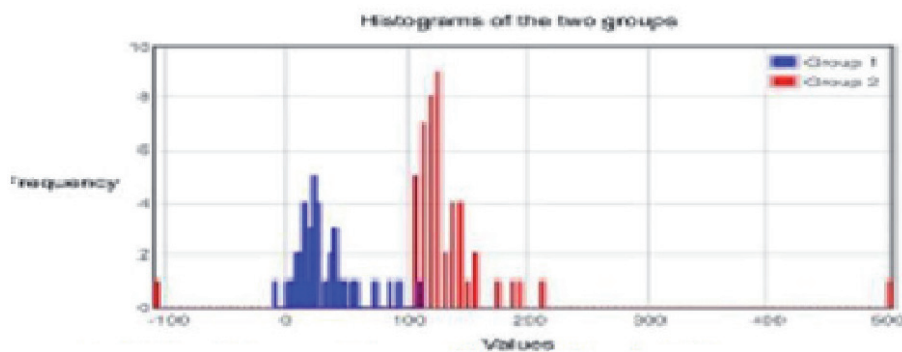


Figure 9.
The difference between group 1 Rong's ratio group 2 Dr. V. Siva's modification.

sugar level of 150 mg/dl. The delayed PETCT was done Four hours after the post injection time with voluntary consent of the patients without any additional injection of the tracer or contrast medium. The SUV max values were obtained utilizing the Advantage 4.4 software provided by the GE. Total of Forty eight lymph nodes at various locations were included in the study. The calculated SUV max values were used to arrive at the Rong's Retention Ratio and the Dr. V. Siva's modification of RRI.

The Rong's retention ratio in the Metastatic lymph nodes group showed the mean value of 37.2 ± 17.0 . Dr. V. Siva's modification of the Rong's Ratio showed the mean value of 132.7 ± 19.8 . The Dr. V. Siva's modification of Rong's Retention ratio resulted in the increase in value by 100 with no significant overlap.

In the previous study of dual PETCT scintimetric characterization of the various primary malignancies the Rong's Retention ratio showed the mean value of 35.8 ± 8 and the Dr. V. Siva's modification of RRI showed the mean value of 135 ± 8.1 as reported confirming that the definitive cut of value of 100 and above could be assigned to indicate the malignant and metastatic lesions in the Dual Phase PETCT scans in the Dr. V. Siva's modification method. By eliminating the subtraction of early SUV max value from the delayed SUV max value the negative values were avoided. The statistical analysis of the data using student t test evaluation showed that there is clear cut demarcation between the original Rong's Retention Ratio values and the Dr. V. Siva's modification of Rong's Ratio as shown in the **Figure 9**.

The p value is < 0.0001 indicating the validity of Dr. V. Siva's modification of Rong's Ratio in the Scintimetric characterization of the metastatic lymph nodes of various primary cancers. However the homogeneous population of cancer patients and non-inclusion of the benign lymph nodal enlargement is a definitive limitation of this study. Further evaluation of this concept is warranted as this is a single institutional study of short duration and small number of cases.

10. Conclusions

The Scintimetric Characterization of the skeletal hot spots helps in the differentiation of benign and malignant lesions that might coexist in a carcinoma prostate patient and treat them accordingly. This has been proved to be useful in the assessment of non healing fractures and pathological fractures as well. The usefulness of this in the evaluation of Rheumatoid Arthritis opens up a new era of research on clinical utilization in both the diagnostic and prognostic aspects of the disease process. The identification and characterization of the diastolic dysfunction directly by applying the Systolic/Diastolic count ration in the gated SPECT myocardial viability studies remains to be explored further.

The advent and quantification of FDG uptake in a hot spot in the Dual Phase PETCT scan helps in the identification and differentiation of various primary malignant processes and the Metastatic involvement of the lymph nodes. The clinical application of the quantitative indices like the Israel's ratio, Dr. V. Siva's retention ratio in the conventional nuclear medicine studies must see the light of clinical utilization of day to day practice. Similarly in the case of PETCT evaluation of Oncology the utilization of the Rong's retention ratio and the Dr. V. Siva's modification of Rong's Ratio should reach the daily practice mode from the bench [50–52].

11. Future perspectives

In the current era of large volume Data handling and DATAMATIC scenario this quantitative approach will be more suitable for the QBOT establishment for qualitative standardization of the Nuclear Medicine studies [53]. These quantitative indices can be incorporated into the automatic report generation aspect of the Artificial Intelligence in Nuclear medicine as reported by Cumali Aktolun and Felix Nensa [54, 55]. The recent explosion in DATA sciences and ARTIFICIAL INTELLIGENCE provide a new arena worth exploring in the future.

Conflict of interest

The authors declare no conflict of interest.

Notes/thanks

The authors express their gratitude and fervent references at the divine lotus feet of Bhagawan Sri Sathya Sai Baba varu with whose sole blessings alone this work had become a reality.

Author details


V. Sivasubramaniyan^{1,2*} and K. Venkataramaniah¹

¹ Department of Physics, Sri Sathya Sai Institute of Higher Learning, Puttaparthi, Andhra Pradesh, India

² Department of Nuclear Medicine, Sri Aurobindo Institute of Medical Sciences, Indore, Madhya Pradesh, India

*Address all correspondence to: drvssm@gmail.com

IntechOpen

© 2021 The Author(s). Licensee IntechOpen. This chapter is distributed under the terms of the Creative Commons Attribution License (<http://creativecommons.org/licenses/by/3.0>), which permits unrestricted use, distribution, and reproduction in any medium, provided the original work is properly cited. 

References

- [1] Rosenthal L, Kaye M (1975) Technetium 99m pyrophosphate kinetics and imaging in metabolic bone disease. *J Nucl Med* 16:33-39.
- [2] Lentle BC, Russell AS, Percy JS, Jackson FI (1977) The scintigraphic investigation of sacroiliac disease *J Nucl Med* 18:529-533.
- [3] Condon BR, Buchanan R, Garvie NW et al (1981) Assessment of secondary bone lesions following cancer of the breast or prostate using serial radionuclide imaging. *Br. J Radiol* 54:18-23.
- [4] Vellenga CJLR, Pauwels EKJ, Bijvoet OLM (1984) Comparison between visual assessment and quantitative measurement of radioactivity on the bone scintigram in Paget's disease of bone. *Eur J Nucl Med* 9:533-537.
- [5] Pfeifer JP, Hill W, Bull U, Burkhardt R, Kirsch CM (1983) Improvement of bone scintigraphy by quantitative evaluation compared with X-ray studies and iliac crest biopsy in malignant disease. *Eur J Nucl Med* 8: 342-345.
- [6] Constable AR, Cranage RW (1980) Recognition of superscan in prostatic bone scintigraphy. *Br J Radiol* 54: 122-125.
- [7] Hardy JG, Kulatilake AE, Wastie ML (1980) An index for monitoring bone metastases from carcinoma of the prostate. *Br J Radiol* 53: 869-873.
- [8] Mendiok H, Rapoport A, Oreopoulos DG, Rabinovich S, Meema HF, Meema S (1985) Quantitative radionuclide scanning in metabolic bone disease. *Nucl Med Comm* 6: 141-148.
- [9] Israel O, Front D, Frenkel A, Kleinhaus U (1985) 24 hour/4 hour ratio of technetium 99m methylene diphosphonate uptake in patients with bone metastases and degenerative bone changes. *J Nucl Med* 26: 237-240.
- [10] V. Sivasubramanian and K. Venkataramaniah, Temporal Scintimetric Characterization of Skeletal Hotspots in Bone Scan by Dr. V. Siva's Retention Ratio S.C. Satapathy et al. (eds.), *Information Systems Design and Intelligent Applications, Advances in Intelligent Systems and Computing* 433, DOI 10.1007/978-81-322-2755-7_31
- [11] Langsteger W, Haim S, Knauer M, Waldenberger P, Emmanuel K, Loidl W, Wolf I, Beheshti M. Imaging of bone metastases in prostate cancer: An update. *Q J Nucl Med Mol Imaging*. 2012 Oct; 56(5):447-458.
- [12] Brian C. Lentle, M.D., F.R.C.P. (C); Anthony S. Russell, M.B., F.R.C.P (C); John S. Percy, M.D., F.R.C.P. (Edin) (C); John R. Scott, M.Sc.; and Frank I. Jackson, M.B., C.R.C.P. (C) *Bone Scintiscanning Updated*. (*Ann Intern Med*. 1976; 84(3):297-303. doi:10.7326/0003-4819-84-3-297.
- [13] Batson OV: The function of the vertebral veins and their role in the spread of metastases. *Clin Orthop Relat Res* 312: 4-9, 1995.
- [14] Paget S: The distribution of secondary growths in cancer of the breast. *Cancer Metastasis Rev* 8: 98-101, 1989.
- [15] Masuda H, Fukabori Y, Nakano K, Takezawa Y, T CS and Yamanaka H: Increased expression of bone morphogenetic protein-7 in bone metastatic prostate cancer. *Prostate* 54: 268-274, 2003.
- [16] De Pinieux G, Flam T, Zerbib M, Taupin P, Bellahcene A, Waltregny D, Vieillefond A and Poupon MF: Bone

sialoprotein, bone morphogenetic protein 6 and thymidine phosphorylase expression in localized human prostatic adenocarcinoma as predictors of clinical outcome: A clinicopathological and immunohistochemical study of 43 cases. *J Urol* 166: 1924-1930, 2001.

[17] Shariat SF, Shalev M, Menesses-Diaz A, Kim IY, Kattan MW, Wheeler TM and Slawin KM: Preoperative plasma levels of transforming growth factor beta(1) (TGF-beta(1)) strongly predict progression in patients undergoing radical prostatectomy. *J Clin Oncol* 19: 2856-2864, 2001.

[18] Klaus Strobel, Cyrill Burger, Burkhardt Seifert, Daniela B. Husarik, Jan D. Soyka1, Thomas F. Hany Characterization of Focal Bone Lesions in the Axial Skeleton: Performance of Planar Bone Scintigraphy Compared with SPECT and SPECT Fused with CT *AJR*: 188, 467-474, May 2007.

[19] Lehr JE and Pienta KJ: Preferential adhesion of prostate cancer cells to a human bone marrow endothelial cell line. *J Natl Cancer Inst* 90: 118-123, 1998.

[20] Sivasubramaniyan V* and Venkataramaniah K, Non-invasive Quantitative Characterization of Skeletal Metastasis in Carcinoma Prostate by Tc99m MDP Bone Scans Using Dr. V. Siva's Retention Ratio in Correlation with Serum PSA Levels, *Med Surg Urol* Volume 5 Issue 2 1000164

[21] Rahul Namdeo, Dr. V. Sivasubramaniyan, Dr. K. Vijaya Sai, Dr. K. Venkataramaniah Scintimetric Evaluation in the Assessment of Delayed Union of Skeletal Fractures, *International Journal of Innovative Research and Development*, www.ijird.com July, 2015 Vol 4 Issue 8.

[22] Sivasubramaniyan n, Venkataramaniah K, Comparative

Evaluation of the role of Scintimetric Characterization by Dr. V. Siva's Retention Ratio and the Triple Phase Bone Scan in the Skeletal Fracture Assessment. *J Trauma Treat* 7: 421. doi:10.4172/2167-1222.1000421, 2018.

[23] Sivasubramaniyan V. K Venkataramaniah. Scintimetric Characterization of Skeletal Hotspots by Dr. V. Siva's Retention Ratio in A Diagnostic Referral Center. *Biomed J Sci and Tech Res* 6(5)2018. BJSTR. MS.ID.001420. DOI: 10.26717/BJSTR.2018.06.001420.

[24] Sivasubramaniyan V and Venkataramaniah K, Scintimetric Evaluation of the Rheumatoid Arthritis Involvement by Dr. V. Siva's Retention Ratio-(Preliminary Report). *J Arthritis* 6: 231. doi:10.4172/2167-7921.1000231 2017.

[25] Sherif F. Nagueh, Christopher P. Appleton, Thierry C. Gillebert, Paolo N. Marino, Jae K. Oh, Otto A. Smiseth, Alan D. Waggoner, Frank A. Flachskampf, Patricia A. Pellikka, Arturo Evangelisa. Recommendations for the evaluation of left ventricular diastolic function by echocardiography – Houston, Texas; Phoenix, Arizona; Ghent, Belgium; Novara, Italy; Rochester, Minnesota; Oslo, Norway; St. Louis, Missouri; *European Journal of Echocardiography*. 2009;10:165-193.

[26] Thomas Mathew, Rick Steeds, Richard Jones, Prathap Kanagala, Guy Lloyd, Daniel Knight, Kevin O' Gallagher, David Oxborough, Bushra Rana, Liam Ring, Julie Sandoval, Gill Whart, Richard Wheeler. A guideline protocol for the echocardiographic assessment of diastolic dysfunction. Published November; 2013.

[27] Juan Lacalzada, et al. Evaluation of left ventricular diastolic function by echocardiography. *Hospital Universitario de Canarias, La Laguna, Santa Cruz de Tenerife* Chapter 6,

Establishing Better Standards of Care in Doppler Echocardiography, Computed Tomography and Nuclear Cardiology Edited by Dr. Richard M. Fleming; 2011.

[28] Morgan MG, Mannting F, et al. Gated SPECT with Tc99m SESTAMIBI for assessment of myocardial perfusion abnormalities. JNM. 1993;21:13.

[29] Raymond Taillefer, Gordon Dupey E, et al. Comparison between end diastolic and the summed images of gated Tc99m MIBI SPECT in the detection of C.a.D in women. JNC; 1999.

[30] Depuey EG, Nicholas K, et al. Left ventricular ejection fraction assessed from gated Tc99m sestamibi SPECT. JNM. 1993;34.

[31] Sivasubramaniyan V, Dash PK, Iyer VR, Prasad RD, Purantharan N. Role of gated SPECT myocardial perfusion imaging in the evaluation of diastolic dysfunction of the heart oral. Paper Presentation Session 1 (Parallel) (Cardio Vascular System) Abstracts of SNMICON; 2003.

[32] Ichiro Nakae, Shinro Matsuo, Terue Koh, Kenichi Mitsunami, Minoru Horie. Left ventricular systolic/diastolic function evaluated by quantitative ECG-gated SPECT: Comparison with echocardiography and plasma BNP analysis. Annals of Nuclear Medicine. 2005;19(6):447-454.

[33] Cigdem Akincioglu, Daniel S. Berman, Hidetaka Nishina, Paul B. Kavanagh, Piotr J. Slomka, Aiden Abidov, Sean Hayes, John D. Friedman, Guido Germano. Assessment of diastolic function using 16Frame 99mTc-Sestamibi gated myocardial perfusion SPECT: Normal values. J Nucl Med. 2005;46:1102-1108.

[34] Lele KarunaLuthra, Yogini Sawant. Assessment of diastolic heart function – Experience with 16-gated myocardial

perfusion SPECT RD. JAPI. 2008;56:763-767.

[35] Vakili BA, Okin PM, Devereux RB. Prognostic implications of left ventricular hypertrophy. American Heart Journal. 2001;141(3):334-341.

[36] Agabiti-Rosei E, Muiesan ML. Left ventricular hypertrophy and heart failure in women. Journal of Hypertension. Supplement: Official Journal of the International Society of Hypertension. 2002;20(2):S34.

[37] Torpy JM, Lynm C, Glass RM. JAMA patient page. JAMA. 2010;303(15).

[38] Woodiwiss AJ, Norton GR. Obesity and left ventricular hypertrophy: The hypertension connection. Current Hypertension Reports. 2015;17(4):28.

[39] Di Lullo L, Gorini A, Russo D, Santoboni A, Ronco C. Left ventricular hypertrophy in chronic kidney disease patients: From pathophysiology to treatment. Cardiorenal Medicine. 2015;5(4):254-266.

[40] Shah AS, Chin CW, Vassiliou V, Cowell SJ, Doris M, Kwok TN, Semple S, Zamvar V, White AC, McKillop G, Boon NA. Left ventricular hypertrophy with strain and aortic stenosis. Circulation. 2014;130(18):1607-1616.

[41] Tsai SY, Wang SY, Shiau YC, Wu YW. Mechanical dyssynchrony and diastolic dysfunction are common in LVH: A pilot correlation study using Doppler echocardiography and CZT gated-SPECT MPI. Scientific Reports. 2018;8(1):1-2.

[42] Kubota K, Itoh M, Ozaki K, et al. Advantage of delayed whole-body FDG-PET imaging for tumour detection. Eur J. Nucl Med. 2001;28:696-703.

[43] Chen YM, Huang G, Sun XG, et al. Optimizing delayed scan time for FDG

- PET: Comparison of the early and late delayed scan. *Nucl Med Commun.* 2008;29:425-430.
- [44] Rong Tian, Minggang Su, Ye Tian, Fanglan Li, Lin Li, Anren Kuang, Jiancheng Zeng. Dual-time point PET/CT with F-18 FDG for the differentiation of malignant and benign bone lesions. *Skeletal Radiol.* 2009;38:451-458.
- [45] Griffith LK. Use of PET/CT scanning in cancer patients: Technical and practical considerations. In *Baylor University Medical Center proceedings.* Taylor and Francis. 2005;18(4):321-330.
- [46] Sachpekidis C, Thieke C, Askoxylakis V, Nicolay NH, Huber PE, Thomas M, Dimitrakopoulou G, Debus J, Haberkorn U, Dimitrakopoulou-Strauss A. Combined use of 18F-FDG and 18F-FMISO in unresectable non-small cell lung cancer patients planned for radiotherapy: A dynamic PET/CT study. *American Journal of Nuclear Medicine and Molecular Imaging.* 2015;5(2):127.
- [47] Li K, Sun H, Guo Q. Combinative evaluation of primary tumor and lymph nodes in predicting pelvic lymphatic metastasis in early-stage cervical cancer: A multiparametric PET-CT study. *European Journal of Radiology.* 2019;113:153-157.
- [48] Du S, Sun H, Gao S, Xin J, Lu Z. Metabolic parameters with different thresholds for evaluating tumor recurrence and their correlations with hematological parameters in locally advanced squamous cell cervical carcinoma: An observational 18F-FDG PET/CT study. *Quantitative Imaging in Medicine and Surgery.* 2019;9(3):440.
- [49] den Hoff J, Hofheinz F, Oehme L, et al. Dual time point based quantification of metabolic uptake rates in 18F-FDG PET. *EJNMMI Res.* 2013;3:1-6.
- [50] Jones C, Badger S, Lynch T. A potential diagnostic role of dual phase 18F-FDG PET/CT scanning. *Ulster Med J.* 2014;83:52-54.
- [51] Dr. V. Sivasubramaniyan, Sai Shivnarayan, Dr. K. Venkataramaniah, Scintimetric Characterization of Primary Tumors by Dual Phase PETCT study, *INDIAN JOURNAL OF APPLIED RESEARCH*, Feb. 2020. Volume 10/ Issue 2/61-62
- [52] Dr. V. Sivasubramaniyan, Dr. Vinod Bhandari, Dr. K. Venkataramaniah, Scintimetric Characterization of metastatic lymph nodes in various primary malignancies by Dual Phase PETCT study, *MODERN APPLIED MEDICAL RESEARCH* 1(1): 01-03
- [53] Nagy et al. *EJNMMI Physics* (2021)8:2. doi:10.1186/s40658-021-00371-w
- [54] Cumali Aktolun, Artificial intelligence and radiomics in nuclear medicine: Potentials and challenges, *European Journal of Nuclear Medicine and Molecular Imaging* (2019) 46:2731-2273. doi:10.1007/s00259-019-04593-0
- [55] Felix Nensa¹, Aydin Demircioglu¹, and Christoph Rischpler², Artificial Intelligence in Nuclear Medicine, *THE JOURNAL OF NUCLEAR MEDICINE* Vol. 60 No. 9 (Suppl. 2) September 2019.